

1 Development of high resolution linear-cut beam position monitor
2 for heavy-ion synchrotron of KHIMA project

3 Ji-Gwang Hwang^{a,b}, Tae-Keun Yang^a, Peter Forck^c, Seon Yeong Noh^a, Garam Hahn^a, Minkyoo Choi^a

4 ^aKorea Institute of Radiological and Medical Sciences, 215-4, Gongneung-dong, Nowon-gu, Seoul, 139-706, Korea

5 ^bHelmholtz-Zentrum Berlin (HZB), Albert-Einstein-straße 15, 12489 Berlin, Germany

6 ^cGSI Helmholtz Centre for Ion Research, 64291 Darmstadt, Germany.

7 **Abstract**

A beam position monitor with high precision and resolution is required to control the beam trajectory for matching to the injection orbit and acceleration in a heavy-ion synchrotron. It will be also used for measuring the beta function, tune, and chromaticity. Since the bunch length at heavy ion synchrotron is relatively long, a few meters, a boxlike device with plates of typically 20 cm length is used to enhance the signal strength and to get a precise linear dependence with respect to the beam displacement. Especially, the linear-cut beam position monitor is adopted to satisfy the position resolution of 100 μm and accuracy of 200 μm for a nominal beam intensity in the KHIMA synchrotron of $\sim 7 \times 10^8$ particles for the carbon beams and $\sim 2 \times 10^{10}$ for the proton beams. In this paper, we show the electromagnetic design of the electrode and surroundings to satisfy the resolution of 100 μm , the criteria for mechanical aspect to satisfy the position accuracy of 200 μm , the measurement results by using wire test-bench, design and measurement of a high input impedance pre-amplifier, and the beam-test results with long ($\sim 1.6 \mu\text{s}$) electron beam in Pohang accelerator laboratory (PAL).

8 **Keywords:** Linear-cut beam position monitor, heavy-ion synchrotron, medical accelerator

9 **1. Introduction**

10 The main purpose of the Korea Heavy Ion Medical Accelerator (KHIMA) project is to construct a
11 proton and carbon therapy accelerator based on a synchrotron currently under construction in Korea [1].
12 Low intensity proton and carbon beams with energies in the range of 110 to 430 MeV/u for a carbon beam
13 and 60 to 230 MeV for a proton, which corresponds to a water equilibrium beam range of 3.0 to 27.0 g/cm²,
14 are produced by the accelerator for a cancer therapy [2]. The accelerator consists of the low energy beam
15 transport (LEBT) line, radio-frequency quadrupole (RFQ), interdigital H-mode drift-tube-linac (IH-DTL),
16 medium beam transport (MEBT) line, synchrotron, and high energy beam transport (HEBT) line [3]. The
17 circumference of the synchrotron is about 75 m designed for an injection energy of the carbon and proton
18 beams of 7 MeV/u. This corresponds to the revolution frequency of 0.487 MHz. The revolution frequency
19 is ramped from 0.487 MHz at 7 MeV/u to ~ 3 MHz at 430 MeV/u for carbon and 230 MeV for proton.

20 In the KHIMA synchrotron, a high precision beam position monitor, which has a position resolution
21 and accuracy of 100 μm and 200 μm , respectively, is required to match and control the beam trajectory
22 during beam injection and acceleration [4]. It is also used for measuring the closed orbit, Twiss parameters,
23 betatron tunes, and chromaticity in the synchrotron. Since the multi-turn injection, the so called painting
24 method, is adopted for reducing the operation cost by increasing the beam intensity in the synchrotron
25 during one cycle, the longitudinal distribution of the ion beam is fully filled as like a DC beam current at
26 the initial stage and it is bunched after the capturing process using magnetic alloy cavity.

27 The bunch length in the heavy ion synchrotron is relatively long, a few meters, and the intensity of the
28 beam is low, a box-like beam position monitor (BPM) with long plates of typically 20 cm is used to enhance
29 the signal strength and to obtain a precise linear dependence with respect to the beam displacement [7].
30 The number of the separately installed horizontal and vertical beam position monitors in the synchrotron

³¹ is 10 and 7, respectively. The position of the monitor is determined based on the amplitude of the betatron
³² oscillation [6]. The layout of KHIMA is shown in Fig. 1.

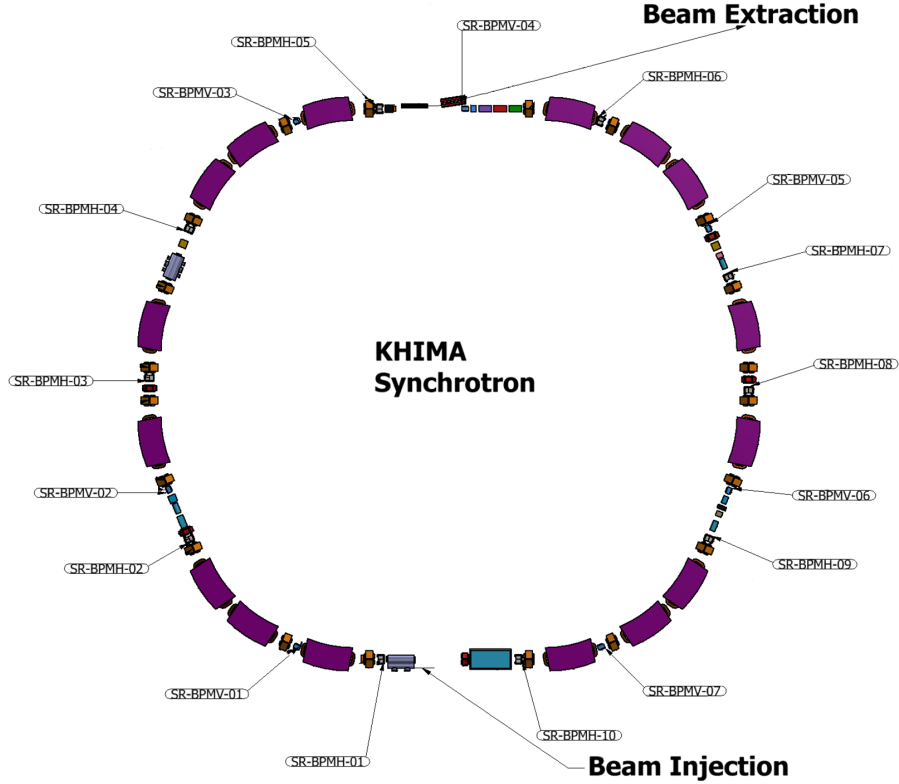


Figure 1: KHIMA synchrotron for cancer therapy using a low intensity beams with an energy in range of 110 to 430 MeV/u for a carbon beam and 60 to 230 MeV for a proton [3]. RF frequency of magnetic alloy cavity is increased from 0.487 to 3 MHz as follow beam velocity in the synchrotron. The SR-BPMV and SR-BPMH are presented the vertical and horizontal linear-cut beam position monitors, respectively, in the synchrotron.

³³ 2. Electromagnetic and mechanical design of linear-cut beam position monitor

³⁴ Since the beam intensity in the synchrotron after the injection and capturing process is low, $\sim 7 \times 10^8$
³⁵ particles for the carbon beams and $\sim 2.1 \times 10^{10}$ for the proton beams [4], the design of the beam position
³⁶ monitor yielding a position resolution of $100 \mu\text{m}$ and accuracy of $200 \mu\text{m}$ is intended. The linear-cut beam
³⁷ position monitor was chosen to satisfy these requirements [7]. It consists of two copper electrodes, the body
³⁸ for maintain the structure of the electrode, holders to combine the body with the vacuum chamber, and the
³⁹ vacuum chamber. It can be consider as a capacitive pick-up device. The induced image charge of the beam
⁴⁰ is coupled via a resistor on an amplifier for further processing. The induced voltage drop at a resistor R
⁴¹ is [7]

$$V(\omega) = Z_t(\omega, \beta) I_{beam}(\omega) = \frac{1}{\beta c} \frac{1}{C} \frac{A}{2\pi a} \frac{i\omega RC}{1 + i\omega RC} I_{beam}(\omega), \quad (1)$$

⁴² where Z_t is longitudinal transfer impedance, $\beta = v/c$, v is the speed of the ions, c is the speed of light, C
⁴³ is the capacitance of the electrode which is depended on mainly the distance between the electrode and the
⁴⁴ vacuum chamber wall, A is the area of the electrode, a is the distance from the beam center to the electrode,

45 ω is the angular frequency, and $I_{beam} = I_0 e^{i\omega t}$ is the current distribution of the beam. The longitudinal
 46 transfer impedance $Z_t(\omega, \beta)$ describes the effect of the beam on the pick-up voltage. It is dependent on
 47 frequency, on the velocity of the beam particles and on geometrical factors. The transfer impedance, which
 48 is inversely proportional to the capacitance and ion beam velocity and is proportional to the area of the
 49 electrode, input impedance of the amplifier and operating frequency, determines the signal strength of the
 50 beam position monitor. The transverse and longitudinal size is restricted because the beam position monitor
 51 would be installed inside the steering magnet yoke to conserve the space. The width and thickness of two
 52 electrodes are determined to 136 mm and 2 mm, respectively. The thickness of the body is determined to 5
 53 mm to reduce the distortion of the electrodes. The distance between the body and electrode is maintained
 54 to be 8 mm to increase the induced signal by reducing the capacitance. The copper bolts are welded on
 55 the electrodes surface to assemble with the body without the holes on electrodes. The screws have a central
 56 hole through the body of the screw to serve as a vent, allowing trapped gas to escape from a blind hole
 57 when a vacuum chamber is pumped down. The feed-through is welded to the flange and it is inserted into
 58 the vacuum chamber to increase the signal strength by reducing the distance between feed-through and
 59 electrode. The feed-through pin is connected with electrode by the holder made of the beryllium copper
 60 material which has the good elasticity for the good contact. The length of horizontal and vertical beam
 61 position monitor are 290 mm and 244 mm, respectively. The designed horizontal linear-cut beam position
 62 monitor is shown in Fig. 2.

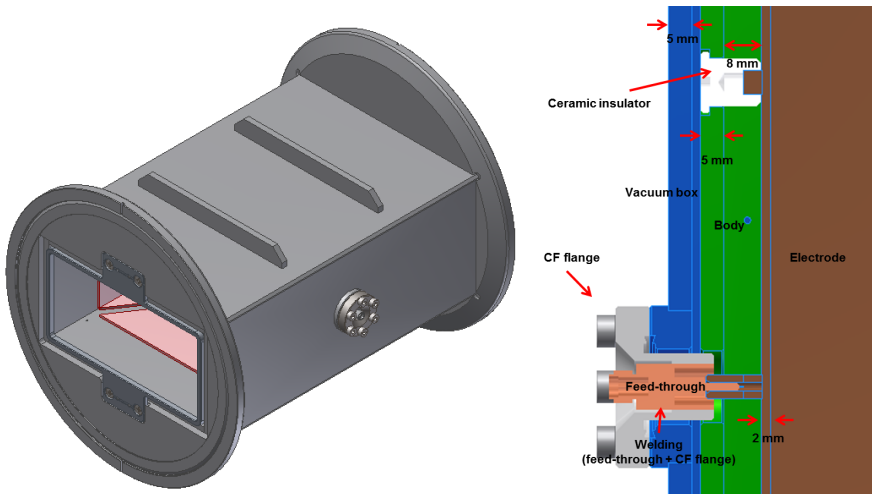


Figure 2: Horizontal linear-cut beam position monitor in KHIMA synchrotron which consists of two copper electrodes with the width of 142 mm, height of 76 mm, and length of 200 mm, metal body, holders, and vacuum chamber. The thickness of vacuum chamber, body, and electrodes are 5 mm, 5 mm, and 2 mm, respectively. The distance between body and electrode is maintained to be 8 mm to increase induced signal by reducing capacitance of the system.

63 Based on the optimized dimensions and beam velocity of $\beta = 0.73\%$ which corresponds to highest carbon
 64 beam energy of 430 MeV/u, the absolute value of the transfer impedance for various input impedances and
 65 schemes as a function of the operating frequency are calculated using Eq. 1 to increase the signal strength
 66 because the signal strength is proportional to the transfer impedance. As shown in Fig. 3, the transfer
 67 impedance for low impedance such as 50Ω and $1 k\Omega$ is linearly proportional to frequency below the cutoff
 68 frequency, $\omega_{cut} = 1/RC$. The transfer impedance above ω_{cut} with the transformer coupling is lower compared
 69 to the high impedance case because the voltage ratio above the cut-off frequency for a transformer is given by
 70 $U_2/U_1 = N_2/N_1$, where U_1 and U_2 are the induced voltage on the beam position monitor and resistor and N_1
 71 and N_2 the windings on the transformer, respectively, with coupling by a transformer with primary windings
 72 N_1 and secondary windings N_2 . Since the beam intensity in the synchrotron is varies from 0.487 MHz to 3.0 MHz, the impedance termination
 73 of $R = 1 M\Omega$ is chosen for the BPM signals leading to the high-pass cut-off frequency $f_{cut} = 1/(2\pi RC) =$
 74

75 1.7 kHz [7] and to achieve the high position resolution by increasing the induced signal strength.

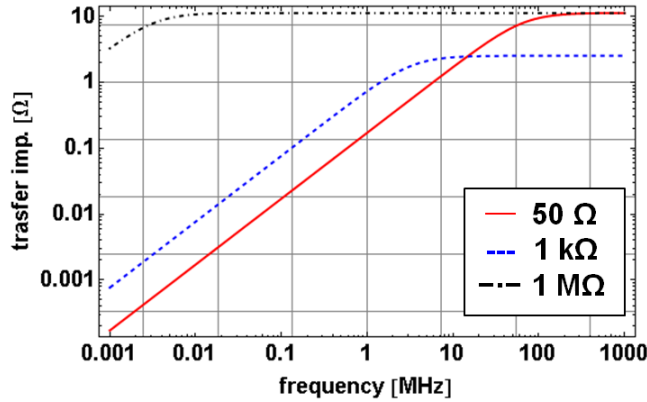


Figure 3: Absolute value of the transfer impedance for capacitance of 183 pF and carbon ion energy of 430 MeV/u ($\beta = 0.73\%$) with 50 Ω (red, solid line) and 1 $M\Omega$ (black, dotdashed line) input impedance amplifier. Third curve (blue, dashed line) is 1 $k\Omega$ impedance using coupling with a winding ratio $N_1/N_2 = 1:20$ and a 50 Ω termination.

76 Since the cross-talk between two electrodes mainly affects the position resolution of the beam position
77 monitor, the cross-talk as function of the distance between two electrodes was investigated to optimize the
78 distance between two electrodes [8]. The result is shown in Fig. 4.

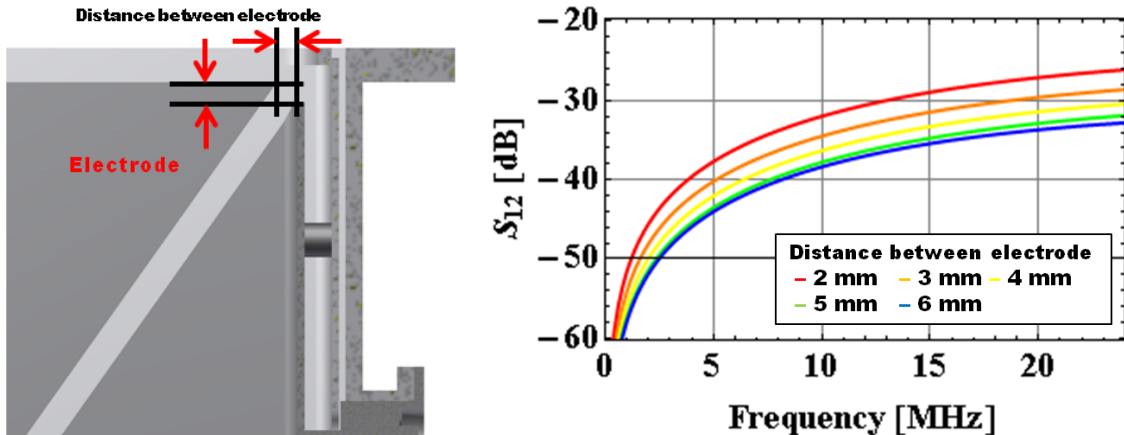


Figure 4: Cross-talk(S_{12}) as a function of distance between two electrodes. The distance between two electrodes is determined to be 6 mm to achieve the cross-talk of less than -40 dB in operating frequency range of 0.487 MHz to 3 MHz.

79 In order to measure the longitudinal distribution using the signal of the beam position monitor, the band-
80 width of the signal processing electronics is chosen to be the tenth harmonics of the accelerating base
81 frequency, up to 30 MHz. Since the beam position is mainly determined by the synchronous frequency
82 component of the signal, the cross-talk, which affects on the misreading of the beam position, is almost to
83 be -40 dB in the frequency range of 0.487 MHz to about 3 MHz when the distance between the electrodes
84 is larger than 5 mm. The signal readout is changed by the cross-talk between two electrode that is given by

$$x + \Delta x = k \frac{((1 - \alpha)U_{left} + \alpha U_{right}) - ((1 - \alpha)U_{right} + \alpha U_{left})}{((1 - \alpha)U_{left} + \alpha U_{right}) + ((1 - \alpha)U_{right} + \alpha U_{left})} = k(1 - 2\alpha) \frac{U_{left} - U_{right}}{U_{left} + U_{right}}, \quad (2)$$

85 where is $\alpha = 10^{S_{12}/20}$ and S_{12} is the cross-talk between two electrodes. The distance between the

86 electrodes is chosen to be 6 mm to achieve the cross-talk of less than -40 dB, which correspond to a position
 87 reading error of about 2 %.

88 In order to confirm the linear response region, resolution and accuracy of the designed beam position
 89 monitor, the induced signals with various beam offsets are calculated by using code CST-PS [11]. From the
 90 computed signals, the ratio of difference and sum of the signals is calculated because the beam position is
 91 determined by the ratio of difference and sum of the signals generated by the two electrodes according to
 92 Eq. 3 [9].

$$x = a_0 \frac{\Delta U}{\Sigma U} + a_1 = a_0 \frac{U_{left} - U_{right}}{U_{left} + U_{right}} + a_1, \quad (3)$$

93 where a_0 is coefficient which is proportional to the transverse dimension of the electrode, a_1 is coefficient
 94 which is related with the electromagnetic central position, the U_{left} and U_{right} are voltage output from the
 95 left and right electrodes, respectively. The the ratio of difference and sum of the signals generated by the
 96 two electrodes, $\Delta U/\Sigma U$, and residuals from the linear fitting curve are shown in Fig. 5 [11].

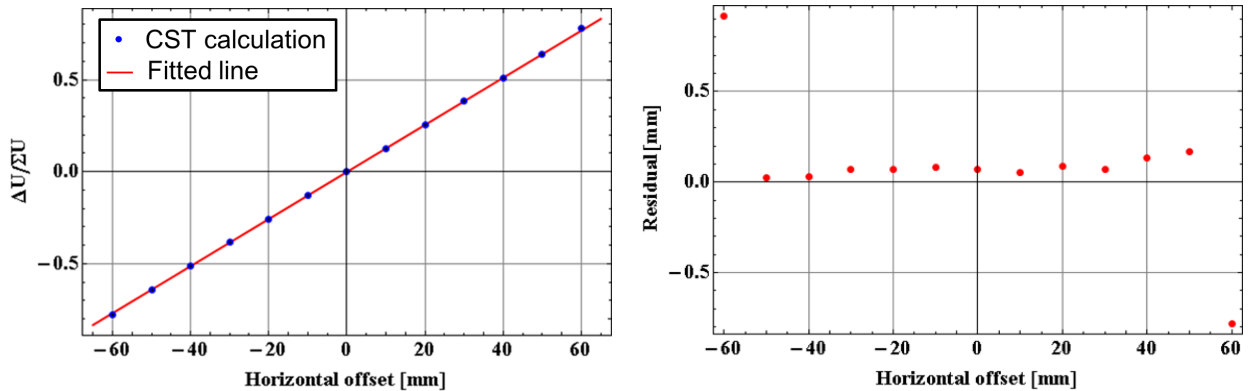


Figure 5: Linearity (left) and residuals (right) of designed beam position monitor calculated by code CST-PS. Designed beam position monitor satisfied position resolution of 100 μ m in range of -40 mm to 40 mm.

97 For the horizontal BPM the ideal values of a_0 and a_1 for the designed beam position monitor from the
 98 dimensions with the width of 142 mm and height of 70 mm are 72 mm and 0 mm, respectively. From the
 99 height limitation of 70 mm, the ideal values of a_0 and a_1 for the vertical beam position monitor are 35 mm
 100 and 0 mm, respectively. Due to the internal structure, such as the insulator and surroundings, the beam
 101 position monitor, however, has the a_0 and a_1 coefficients of 78.10 mm and -72.7 μ m. It is enough to satisfy
 102 the desired position accuracy of 200 μ m.

103 3. Measurement of cross-talk, linearity and calibration factors

104 Based on the results of the electromagnetic and mechanical design, the beam position monitor was
 105 fabricated by the Korean company, I.T.S [12]. The beam position monitor consists of two electrodes, body,
 106 insulator, holder, two feed-through and vacuum chamber. The triangular shape electrodes are made by the
 107 oxygen free copper (OFC), and the body, holder, and vacuum chamber was made of stainless steel, SUS304.
 108 The 99.6 % alumina-ceramic was chosen as the insulator material which was used to attach two electrodes
 109 inside the body with well-defined distance of 8 mm. The special flange from the EVAC is adopted to reduce
 110 the installation space. The required vacuum pressure of 10^{-9} Torr was reached [10]. A photograph of the
 111 fabricated horizontal beam position monitor is shown in Fig. 6.

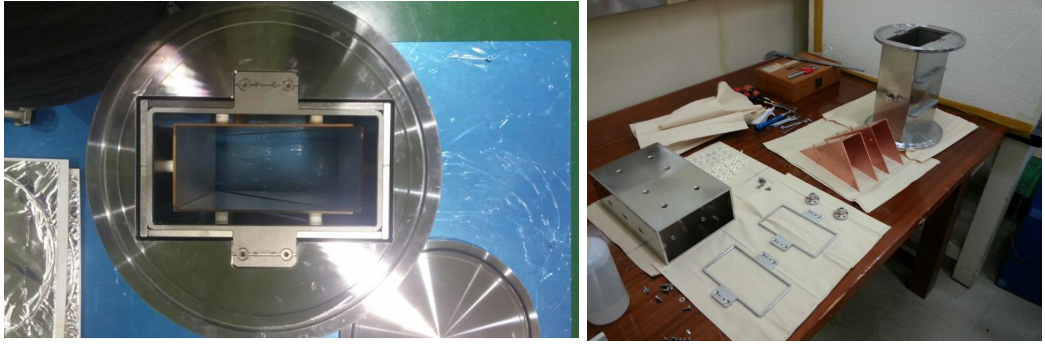


Figure 6: Photograph of fabricated horizontal beam position monitor which consists of two triangular shape copper electrodes, 99.6 % alumina-ceramic insulators, stainless steel body, stainless steel holder, and stainless steel vacuum chamber.

112 The crosstalk S_{12} between two electrodes was measured by using a Vector Network Analyzer, Hewlett
 113 Packard 8753C (Bandwidth : 300 kHz to 3 GHz). The crosstalk is a phenomenon through which a signal
 114 transmitted on one channel creates an undesired effect in another channel. The crosstalk is usually caused
 115 by undesired capacitive or inductive coupling between two channels. The measurement result is shown in
 116 Fig 7 in comparison to the calculation result of CST-MWS [11].

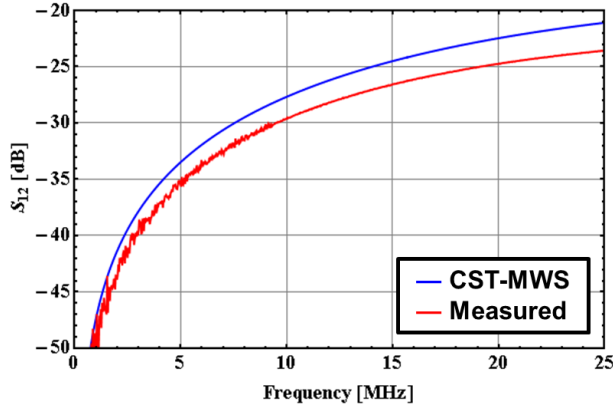


Figure 7: Measured (red) and calculated (blue) cross-talk (S_{12}) of fabricated beam position monitor. Measured cross-talk between two electrodes is lower than -40 dB in range of operation frequency, $0.487 \sim 3$ MHz

117 The measured cross-talk is lower than the -40 dB in the range of operation frequency, $0.487 \sim 3$ MHz,
 118 which is required to achieve the desired position resolution. The measurement result agrees well with the
 119 calculation result using code CST-MWS. The difference between the numerical calculation result using
 120 the CST-MWS and measurement is caused by the residual stray capacitance due to the misalignment of
 121 electrodes.

122 The signal response as a function of the offset (relative wire position) with the RF frequency of 3 MHz
 123 was measured by using the wire test bench to confirm the linearity of the beam position monitor and the
 124 calibration coefficients. The wire test bench is used to confirm the frequency response and linearity of the
 125 pick-up devices from the external source. It consists of the linear X-Y motion stages and well aligned and
 126 stretched wire with two feed-through on the each side. The impedance of the test bench is calculated from
 127 the measurement result of S-parameter of wire test bench. The forward and reflection power are estimated
 128 by the power transfer theorem.

129 The measured signal has high frequency noise. The high frequency noise signal was filtered by digital
 130 low-pass filter during the data processing. The low-pass filter with hard edge model and cut-off frequency of
 131 10 MHz is applied on the FFT (Fast Fourier Transform) of the measured signal. After filtering, the inverse

132 Fourier transformation is performed. It suppresses all frequencies higher than the cut-off frequency and
 133 leaves smaller frequencies unchanged.

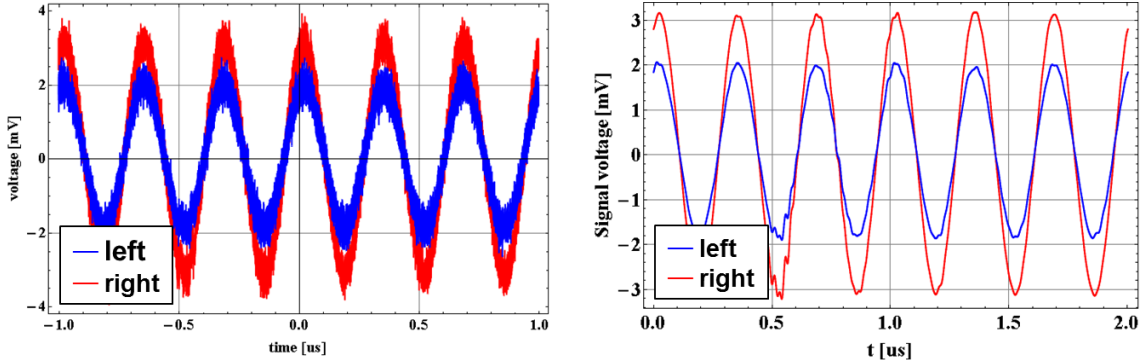


Figure 8: Measured signal (left) by using wire test bench with RF frequency of 3 MHz and its filtered signal (right). High frequency noise is filtered by digital low-pass filter with a cut-off frequency of 10 MHz during data processing.

134 From the signal after the digital low pass filtering process, the $\Delta U/\Sigma U$ is calculated in the offset range
 135 of -28 mm to 28 mm to obtain the calibration coefficients, a_0 and a_1 . The test set-up, the measured result
 136 for linearity, and the obtained calibration factor are shown in Fig. 9.

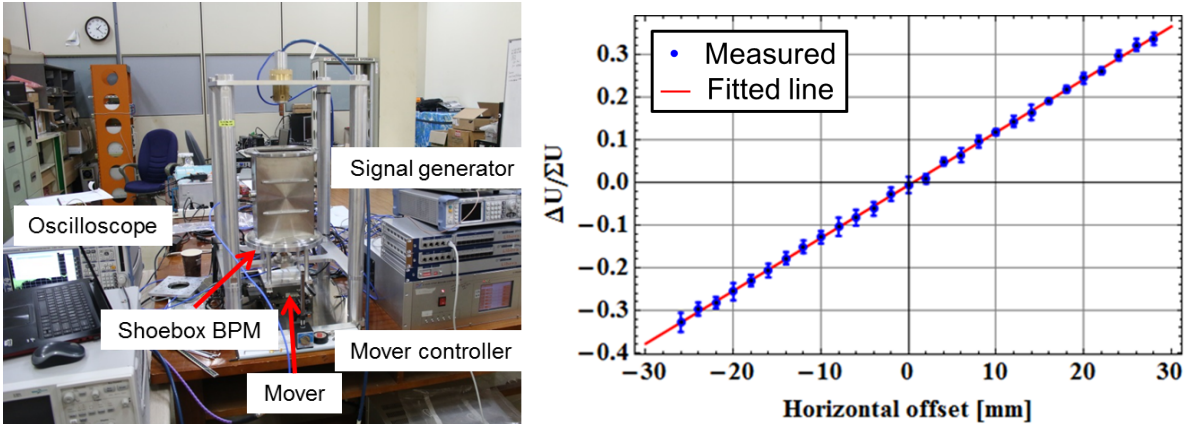


Figure 9: Picture of test set-up by using wire test bench and measurement result of calibration factor and linearity of beam position monitor using wire test bench. The measured calibration coefficients, a_0 and a_1 , are 80.64 mm and 0.475 mm, respectively.

137 The linearity of the beam position monitor in the range of -28 mm to 28 mm was confirmed. The
 138 calibration coefficients of a_0 and a_1 were measured to be 80.64 mm and 475 μ m, respectively. It agrees well
 139 with the calculated value using CST-PS.

140 4. Pre-amplifier design and test

141 The pre-amplifier for amplifying the signal strength from the beam position monitor was designed. It
 142 will be installed close to the beam position monitor, \sim 15 cm long, inside the tunnel to increase the signal
 143 strength by decreasing the capacitance from the cable. It has $1 M\Omega$ input impedance, 40 dB fixed gain,
 144 and bandwidth of $0 \sim 50$ MHz. The bandwidth is determined to be DC \sim 50 MHz to measure the spatial
 145 structure of the beam. The amplifier consists of 2-port RF relay switch and two op-amp. There are two
 146 input ports for each op-amp. One of them is required to confirm the status of the beam position monitor

147 system and calibrate the electronics during the beam operation remotely. It has two individual channels
 148 because the beam position monitor has two signal ports. The switch inside the electronics is controlled using
 149 the DC bias voltage on the two control port (Ctrl1, Ctrl2). It was fabricated by EMWISE in Korea [13].

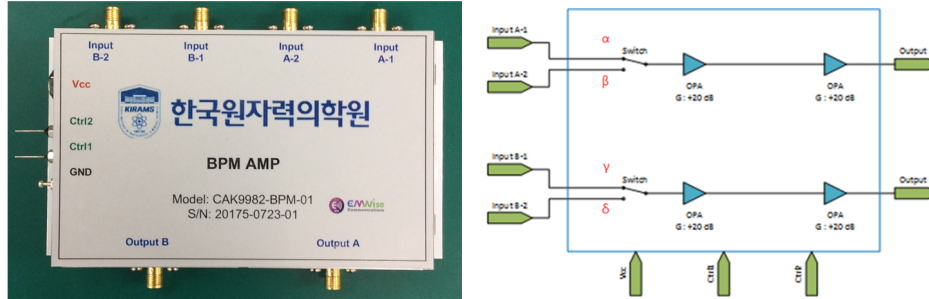


Figure 10: Picture (left) and schematic drawing (right) of 1 M Ω high input impedance pre-amplifier for beam position monitor. It consists of 4 input port for calibration signal and beam signal, 2-port RF relay switch, and two op-ampifiers.

150 The noise figure of the circuit is 9.9 dB for 10 MHz and 9.8 for 50 MHz. The flatness of the gain of
 151 amplifier within the operating frequency is very good to prevent for signal distortions. The gain curve and
 152 S-parameter between input and one output ports as a function of the frequency is measured to confirm the
 153 performance of the pre-amplifier. The gain flatness from a few kHz to 100 MHz was less than ± 0.5 dB.
 154 The result is shown in Fig. 11 and the main parameters are listed on Tab. 1.

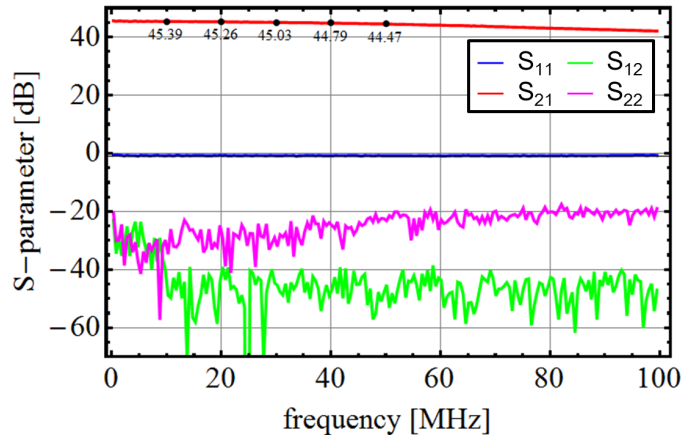


Figure 11: S-parameter of high input impedance pre-amplifier for linear-cut beam position monitor. Gain flatness from a few kHz to 100 MHz is less than ± 0.5 dB and isolation is higher than 20 dB.

155 5. Measurement with electron beam

156 As a preliminary experiment, the beam test with a relativistic electron bunch train, $\sim 1.6 \mu\text{s}$, which
 157 corresponds to the frequency of 630 kHz, is performed at the test LINAC in the Pohang Accelerator Labo-
 158 ratory (PAL). The energy and current of the electron beam are 60 MeV and less than 0.5 mA, respectively.
 159 The 50 MHz cut-off frequency is low enough to collapse the effects of the micro-pulse [14]. A photograph of
 160 the beam test set-up is shown in Fig. 12.

161 The length of the macro-pulse agrees well with the operation frequency, 630 kHz, although the length
 162 of the micro-pulse is very short, less than one nano-second, due to the RF frequency of the S-band LINAC,
 163 2.856 GHz. The beam position monitor is installed on the moving stage to change the relative position of

Table 1: Main parameters of high input impedance pre-amplifier for linear-cut beam position monitor.

Parameter	Unit	Value
Frequency	MHz	DC ~ 50
Input/Output impedance	Ω	1.15 M / 50
Gain	dB	39.5
Gain flatness	dB	± 0.5
Input/Output return loss	dB	24 (min) / 20 (min)
Isolation (Input/Output)	dB	20 (min)
Rejection (Switch)	dBc	80
Noise figure	dB	9.8
Bias voltage/current	V / mA	18 / 114



Figure 12: Picture of beam test set-up with moving stage after beam window at the test LINAC.

the beam position monitor for measuring the calibration factors based on the signal from the beam and the high input impedance amplifier is installed near the beam position monitor to reduce the capacitance from the cable. The collimator made of lead with the diameter of 10 mm and thickness of 30 mm is installed at the entrance of the BPM to prevent the electron hitting the electrode. The gain of the pre-amplifier was 40 dB. The signal as a function of the relative horizontal offset of the moving stage is measured to calculate the calibration factor and to confirm the linear response of the beam position monitor. The measured signal with various horizontal offsets of the moving stage is shown in Fig. 13.

The high frequency noise signal from the surroundings is observed and it is filtered by digital low-pass filter with 1 MHz cut-off frequency during the data processing. The amplitude of the signal is obtained from the filtered signal and $\Delta U/\Sigma U$ as a function offset of the moving stage is calculated to obtain the calibration coefficients, a_0 and a_1 . Those results are shown in Fig. 14.

A non-linear behavior is observed when the offset of the moving stage is large. It may be occurred due to the large beam size and halo particles at the exit of the beam window because the signal strength is decreased when the electron hit the electrode directly. The calibration coefficients of a_0 and a_1 are measured with electron beam to be 79.73 mm and -0.255 mm, respectively. Especially, the a_1 value is not meaningful because the relative central position between the electron beam and position monitor is not defined.

6. Conclusion

The linear-cut beam position monitor was designed, fabricated and tested, which would be installed in the synchrotron ring of KHIMA. The design study of the beam position monitor was performed to achieve the desired position resolution of 100 μm and the accuracy of 200 μm . In order to minimize the distortion and misalignment of the electrodes, the thickness of the body for maintaining the electrodes was optimized. The horizontal beam position monitor was fabricated based on the design values. The laboratory tests,

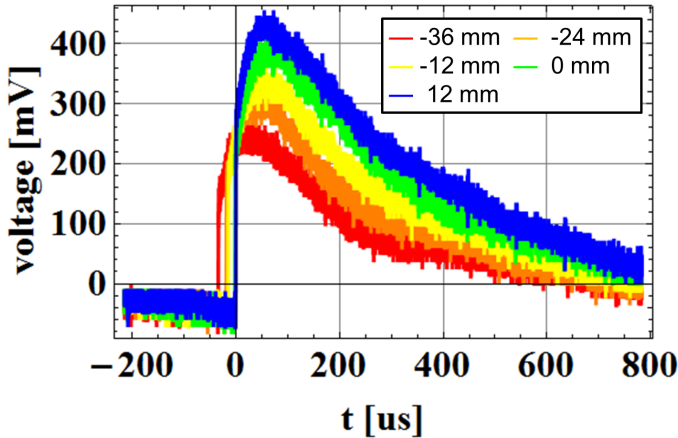


Figure 13: Measured signal with various horizontal offsets of the moving stage.

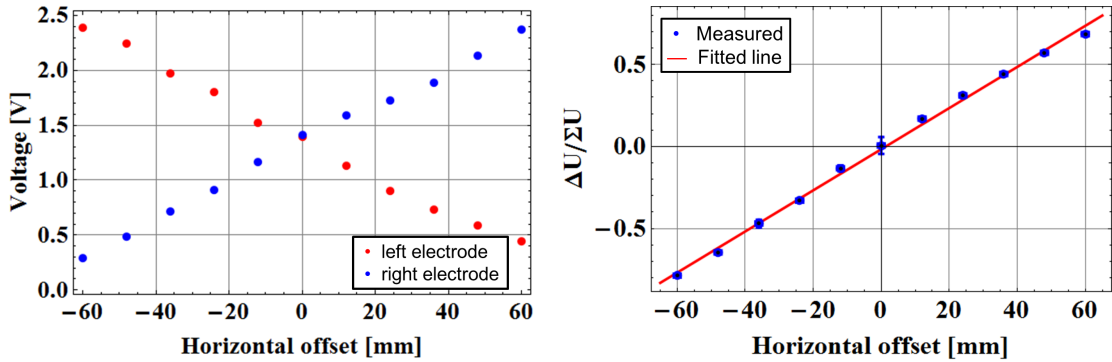


Figure 14: Calibration and linearity measurement of beam position monitor using an electron beam.

such as the vacuum compatibility, the cross-talk measurement and linearity measurement using the wire test bench, were performed to confirm its performance. The measured cross-talk and calibration coefficient agreed well with the designed parameter by the numerical simulation using code CST-MWS and CST-PS. The pre-amplifier was designed and fabricated, of which the input impedance is $1\text{ M}\Omega$ and the fixed gain is 40 dB with ± 0.5 dB flatness in the range of DC ~ 50 MHz. It has two channel and each has two input port for the signal and calibration and it can be switched by the external bias voltage on two pins. The beam test with an electron bunch train at the test LINAC in PAL was performed and the measured calibration coefficients agree with the results of wire test bench.

7. Acknowledgment

The authors wish to thank their collaborators on Pohang Accelerator Laboratory (PAL), Changbum Kim, Dotae Kim, Seung Hwan Shin, and Byung-Joon Lee, for their valuable discussion and encourage for the experiments in test linac of PAL. This work was supported by the National Research Foundation of Korea(NRF) grant funded by the Korea government(MSIP) (no. NRF-2014M2C3A1029534). The beam test was conducted at the test linac operated by Pohang university of science and technology funded by the Ministry of Science, ICT & Future Planning.

References

[1] <http://www.kirams.re.kr/eng/khima>.

- 203 [2] Chawon Park *et al.*, in *The 18th International Conference on Accelerators and Beam Utilization (ICABU2014)* , Daejeon,
204 Korea (2014).
- 205 [3] D. Ahn *et al.*, KHIMA Handbook of Beam Optics for Accelerator System, private communication.
- 206 [4] Heejoong Yim, *The 18th International Conference on Accelerators and Beam Utilization (ICABU2014)* , Daejeon, Korea
207 (2014).
- 208 [5] T. Roser, "Multiturn injection with coupling", *Accelerator division technical note*, TN-354, (1991).
- 209 [6] Heejoong Yim *et al.*, *Journal of the Korean Physical Society*, 67, 1364 (2015).
- 210 [7] P. Forck, *Lecture Notes on Joint University Accelerator School*, Geneva, Switzerland (2011).
- 211 [8] P. Kowina *et al.*, *Proceedings of EPAC2006*, Edinburgh, Scotland, TUPCH013 (2006).
- 212 [9] P. Kowina *et al.*, *Proceedings of DIPAC2005*, Lyon, France, POM033 (2005).
- 213 [10] EVAC website : <http://www.evacvacuum.com/>.
- 214 [11] CST-MWS and PS website : <http://www.cst.com/>.
- 215 [12] I.T.S website : <http://itsvac.com/>.
- 216 [13] EMWISE website : <http://www.em-wise.com/>.
- 217 [14] P. Strehl, *Beam Instrumentation and Diagnostics*, XVII, ISBN 978-3-540-26404-0, Springer, Berlin Heidelberg, Germany
218 (2006).